2023 62nd IEEE Conference on Decision and Control (CDC)
December 13-15, 2023. Marina Bay Sands, Singapore

Economic Model Predictive Control of Water Distribution Systems with Solar Energy and Batteries

Xiangyi Zheng, Ye Wang, Erik Weyer, Chris Manzie

***Abstract*— Pumping in water distribution systems (WDSs) consumes a significant amount of power from the grid and may incur large electricity cost. WDSs with solar panels and batteries can greatly reduce the electricity cost by displacing the use of grid-based electricity with solar or stored energy, while also utilising water storage elements to allow selective pumping. A novel economic model predictive control (EMPC) scheme is proposed in this paper to facilitate optimal operation of pumps, batteries and solar panels in the WDSs. The proposed EMPC controller seeks to minimize the energy cost for water pumping while keeping the water levels in tanks and the battery state of charge within restricted limits. The EMPC is applied to an EPANET model of the Richmond Pruned Network, a Doyle Fuller Newman model of a lithium-ion battery, and simulated output from solar panels to to determine the efficacy of the proposed scheme.**

***Index Terms*— economic model predictive control, water distribution system, solar energy**

I. INTRODUCTION

Water distribution systems (WDSs) play a crucial role in ensuring adequate and timely supply to industrial, agricultural and residential water consumers. Traditionally, WDSs use electricity from the grid to power the pumps, and consequently suffer from huge electricity cost. This makes minimising electricity cost an important objective for water authorities. Previous studies reduced the electricity cost of WDSs by optimizing the pumping schedules based on forecasts of the water demands and the grid electricity prices [1]-[4]. However, cost savings are limited because the grid is the only source of power. To decrease the cumulative electricity cost of WDSs, solar panels can be used as a low cost complementary source of power. The advantage of solar panels compared to other forms of power generation is that they hardly require maintenance, thus having nearly zero cost during operation [6]. Solar panels may be accompanied by lithium-ion batteries so that excess solar energy generated during the day can be stored and used when solar generation is low. Additionally, lithium-ion batteries can store electricity from the grid during off-peak tariff period and supply energy to the network during peak tariff period to lower the energy cost. Similar to solar panels, lithium-ion batteries also have a long lifespan and are free of maintenance [7].

The integration of solar panels and batteries introduces more complexity in operations of WDSs. First, the optimal pumping schedule is influenced by the solar energy generation and the battery storage capacity. Second, the available solar energy needs to be optimally divided between the batteries and the pumps. Finally, water levels in tanks and the battery state of charge need to be restricted based on physical limitations and operational requirements. Therefore, an ideal control strategy needs to be able to handle constraints and provide economically optimal control action in the presence of varying grid electricity prices.

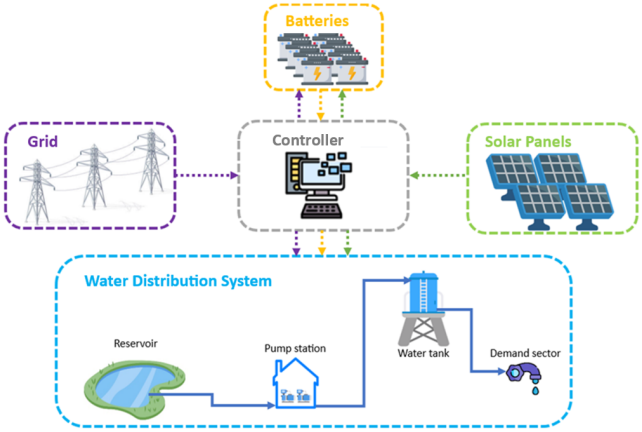

Fig. 1: WDS with local solar energy and batteries, directions and colours of the dotted arrows represent the directions and sources of power flow.

Various control strategies have been applied in WDSs with renewable energy resources. One control strategy for such systems is trigger-level control where pumping and charging actions happen when the water level in a tank and the state of charge of a battery are below certain thresholds [8]. Although this control strategy can tackle constraints, it is not optimal for varying electricity price.

One approach that considers the varying electricity prices is the two-layer control scheme [9] where in the upper layer, a real time optimiser calculates a periodic economic optimal trajectory based on system dynamics and electricity prices, and in the lower layer, a model predictive controller (MPC) with a quadratic stage cost drives the system state onto the trajectory. This approach promises constraint satisfaction and optimal economic operation at steady state, but has no guarantee on optimality during transient.

A more direct approach that does not require a real time optimizer layer is economic MPC (EMPC). This is achieved by using a stage cost that directly measures the economic performance [10]. A key challenge for EMPC is to establish

Xiangyi Zheng, Ye Wang, Erik Weyer, and Chris Manzie are with Department of Electrical and Electronic Engineering at the University of Melbourne. E-mail: xiangyiz@student.unimelb.edu.au, ye.wang1@unimelb.edu.au, ewey@unimelb.edu.au, manziec@unimelb.edu.au.

the true economic cost and constraints for real applications, particularly for systems that have dynamics significantly longer than the MPC horizon.

EMPC has been successfully applied in WDSs and micro-grid systems. In [1] and [2], an EMPC is proposed for optimal operation for WDSs, where the number of pumps operating is used as the input to the system model. The EMPC optimization problem is solved using a mixed integer nonlinear solver to determine the optimal pumping operations. In [3], periodic prices and water demands are used and an EMPC is designed with a periodic terminal constraints to improve close loop stability. In [4], a robust EMPC is designed to tackle the uncertainty in water demand forecast. However, local solar energy and batteries are not considered in their systems. In [11] and [12], EMPC is designed to minimize the cost of electricity in a micro-grids with diesel generator, solar energy and grid energy. It is assumed in [11] and [12], that the power demand is independent of the solar power forecast. However, for WDSs with solar energy and batteries, it is desirable for the pumps to operate during peak solar generation to reduce power cost. This promotes the design of the pump schedule based on the solar power forecast - the power demand of the pumps depends on solar power forecast in this case.

In this paper, we propose an EMPC that minimizes the pumping cost in a low-carbon WDS with behind-the-meter solar energy and batteries. The main contribution is to formulate a new EMPC including a WDS model and the battery model to determine the optimal operations of the pumps, batteries. Then, we apply the proposed EMPC to a simulated system to estimate the potential cost savings available through adoption of the proposed approach under different infrastructure scenarios.

Notation: Subscripts i and j are used to denote Tank i and Pump j. Superscripts s, b, p, g, and d represent solar panels, batteries, pumps, grid, and discharge from the batteries. Superscripts sb, sp, bp, and gb represent the direction of power flow: from solar panels to batteries, from solar panels to pumps, from batteries to pumps, and from grid to batteries. For a variable z, $\overline{z}$ and $\underline{z}$ represent its upper and lower bounds. $k \in \mathbb{Z}$ and $t \in \mathbb{R}$ represent the predicted time step and actual time respectively. For a state variable x, $\widetilde{x}(t)$ represents its true value at time t, and $x(k)$ represents its predicted value at time step k.

II. EMPC FORMULATION

In this section, the control objective of the EMPC is first introduced. Then, the models of the system are developed and the cost function and the constraints are described. Finally, the optimization problem is presented.

A. Control Objective

The main objective of the controller is to minimize the operating cost of a water distribution system with behind-the-meter solar panels and batteries while keeping water levels of storage tanks and states of charge of batteries in restricted ranges. The pump operational cost includes the cost of power drawn from the grid and a cost for pump degradation which is a function of the number of times the pumps are turned ON or OFF. The control inputs are the status of the pumps (ON/OFF for fixed speed pumps), the charging and discharging power of the batteries, and the power drawn from the solar panels. It is assumed that the controller has access to accurate forecasts of water demands, grid energy prices and solar power.

B. System Modeling

For a WDS, the system dynamics in storage tanks can be formulated using volume balances. For a water pumping system with M tanks, let S_i be the base area of tank $i \in [1, M]$, $d_i(k)$ be the total demand supplied by tank i, and $q_i(k)$ be the flow into tank i that is not related to demand (i.e. flow between storage tanks and reservoirs). Then, the dynamics of tank i can be formulated as

$$h_i(k+1) = h_i(k) + \frac{T}{S_i}\left(q_i(k) - d_i(k)\right), \tag{1}$$

where T is the sampling time, $k \in \mathbb{N}$ is the discrete time step. $q_i(k)$ mainly depends on the status of the pumps, but is also influenced by other minor factors such as the change in flow resistance due to the change in flow rate, the change in tank water levels, and the change in water demand [1]. Ignoring those minor factors, a pump-based model for $q_i(k)$ can be written as

$$q_i(k) = \phi_i(n_1(k), \cdots n_m(k)), \tag{2}$$

where m is the total number of pumps in the system, and $n_1(k), \cdots, n_m(k)$ are the operating mode of the pumps. For fixed speed pumps, $n_j(k) \in \{0, 1\}, j = 1, \cdots, m$ can be used to represent the ON-OFF state of the pumps. For variable speed pumps, $n_j(k)$ takes different values for different speeds of the pump.

For the battery, its dynamics can be formulated using the conservation of charge. Let SOC(k) be the state of charge of the battery, C be the maximum capacity of the battery, $P^{sb}(k)$, $P^{gb}(k)$, $P^{d}(k)$, V^{sb}, V^{gb}, V^{d} be the powers and typical voltages for charging the battery from solar panels, the grid and discharging the battery, respectively. The state of charge of battery can be modeled as

$$\begin{aligned}\text{SOC}(k+1) = \text{SOC}(k) + \\ \frac{T}{C}\left(\frac{P^{sb}(k)}{V^{sb}} + \frac{P^{gb}(k)}{V^{gb}} - \frac{P^{d}(k)}{V^{d}}\right).\end{aligned} \tag{3}$$

Remark 1: The terminal voltage of a lithium-ion battery stays relatively constant during charging and discharging unless the battery state of charge is near 0 or 1. Operating near those extreme state of charge conditions causes the battery to degrade much faster, thus is not considered. To prevent the battery from operating near those extreme conditions, limits on the state of charge are formulated in the constraints of the EMPC.

A power balance equation is used to calculate the amount of power drawn from the grid as

$$P^{g}(k) = P^{p}(k) - P^{sp}(k) - P^{bp}(k) + P^{gb}(k), \tag{4}$$

where $P^g(k)$ is the power drawn from the grid, $P^p(k)$ is the pumping power, $P^{sp}(k)$ is the power that the solar panel provides to the pumps, and $P^{bp}(k)$ is the power that the battery provides to the pumps. $P^p(k)$ mainly depends on the status of the pumps and is marginally influenced by water levels in tanks and flow rates through pumps [1]. Ignoring those minor factors, a model for $P^p(k)$ that only depends on the operating modes of the pumps is

$$P^p(k) = \psi(n_1(k), \cdots, n_m(k)). \tag{5}$$

C. Cost Functions and Constraints

To achieve the control objectives, we next build cost functions and constraints. The pumping energy cost at time k can be expressed as

$$l_1(k) = p(k)P^g(k)T, \tag{6}$$

where $p(k)$ is the grid electricity price, and T is the sampling time.

It is undesirable to turn the pumps ON and OFF frequently as this can result in degradation of the pumps. To penalize turning pumps ON or OFF, a cost l_2 is used

$$l_2(k) = \sum_{j=1}^{m} \gamma_j (n_j(k) - n_j(k-1))^2, \tag{7}$$

where γ_j is a weighting factor.

Constraints are introduced to assure the system is operated within the desired limits. Water levels in tanks and the battery state of charge are limited by

$$\underline{h_i} \le h_i(k+1) \le \overline{h}_i, \quad i = 1, \cdots, M, \tag{8a}$$

$$\underline{\text{SOC}} \le \text{SOC}(k+1) \le \overline{\text{SOC}}, \tag{8b}$$

where $\underline{h_i}$ and $\overline{h_i}$ are the lower and upper bounds of the water level in tank i, $\underline{\text{SOC}}$ and $\overline{\text{SOC}}$ are the lower and upper bounds of the battery state of charge. $\overline{h_i}$ is chosen to prevent overflow; $\underline{h_i}$ is chosen to keep a certain amount of water in reserve for unexpected events such as pump failure; $\underline{\text{SOC}}$ and $\overline{\text{SOC}}$ are chosen to assure the battery to operate in the middle range of SOC where the terminal voltage is roughly constant. Note that those constraints are soft constraints and small infrequent violations do not pose major issues.

The pumps are fixed speed pumps and can either be ON or OFF. This is represented by the binary variables

$$n_j(k) \in \{0, 1\}, \quad j = 1, \cdots m, \tag{9}$$

where $n_j(k) = 1$ if that pump j is ON at time k and $n_j(k) = 0$ if that pump j is OFF.

For battery operation, the charging and discharging powers cannot exceed the maximum allowed charging and discharging power. This results in the following constraints:

$$0 \le P^{sb}(k) \le \overline{P}^{sb}, \tag{10a}$$

$$0 \le P^{gb}(k) \le \overline{P}^{gb}, \tag{10b}$$

$$0 \le P^{d}(k) \le \overline{P}^{d}, \tag{10c}$$

where $\overline{P}^{sb}$, $\overline{P}^{gb}$, and $\overline{P}^{d}$ are the maximum allowed power when charging the battery using the solar panels, charging the battery from using the grid, and discharging the battery.

For the operation of solar panels, power cannot be transferred from the pumps back to the solar panels. Moreover, the power from the solar panels can be transferred to the pumps or the battery, or neither of them if no pump is running and the battery is full. This gives the following constraints:

$$P^{sp}(k) \ge 0, \tag{11a}$$

$$P^{sb}(k) + P^{sp}(k) \le P^{s}(k). \tag{11b}$$

Finally, the amount of power transferred to the pumps by the solar panels and the battery cannot exceed the power consumption by the pumps. Further, the amount of power transferred to the pumps from the battery cannot exceed the discharging power of the battery. Therefore, the following constraints are added:

$$P^{sp}(k) + P^{bp}(k) \le P^{p}(k), \tag{12a}$$

$$0 \le P^{bp}(k) \le P^{d}(k). \tag{12b}$$

Moreover, (4), (10b) and (12a) implies that $P^g(k) \ge 0$ so that no power is delivered back to the grid.

D. EMPC Optimization Problem

Let the input be $\mathbf{u}(k) = [n_1(k), \cdots, n_m(k),\ P^{sb}(k),\ P^{gb}(k),\ P^{d}(k),\ P^{sp}(k),\ P^{bp}(k)]$. With a prediction horizon of N, at each time step t, the EMPC solves the following optimization problem:

$$\underset{\mathbf{u}(0),\cdots,\mathbf{u}(N-1)}{\text{minimize}} \quad \sum_{k=0}^{N-1} (l_1(k) + l_2(k)) \tag{13}$$

subject to (1)-(5), (8a)-(12b), $\quad k = 1, \cdots, N-1$

$$h_i(0) = \widetilde{h}_i(t), \quad i = 1, \cdots, M, \tag{14}$$

$$\text{SOC}(0) = \widetilde{\text{SOC}}(t), \tag{15}$$

where (14) and (15) set the initial conditions $h_i(0)$ and $\text{SOC}(0)$ equal to the measured water levels in tanks $\widetilde{h}_i(t)$ and battery state of charge $\widetilde{\text{SOC}}(t)$ at time t. The EMPC optimization problem is nonlinear mixed integer programming due to (2), (5), (7), and (9). If (2) and (5) can be represented by linear expressions, then the optimization problem becomes quadratic programming. Let $\mathbf{u}^*(0)$, $\cdots$, $\mathbf{u}^*(N-1)$ be the solution to the optimization problem, then the optimal control action at time t is chosen as

$$\begin{aligned}\mathbf{u}^*(0) = &[n_1^*(0), \cdots, n_m^*(0), \\ &P^{sb*}(0), P^{gb*}(0), P^{d*}(0), P^{sp*}(0), P^{bp*}(0)].\end{aligned} \tag{16}$$

III. APPLICATION: RICHMOND PRUNED NETWORK

To verify the proposed EMPC, a case study consisting of the EPANET model for Richmond Pruned Network [15], an electrochemical model of a lithium-ion battery, and a solar power source, is presented in this section. The simulation configuration is first introduced. Then, the simulation result

is presented and energy cost savings by the solar panels and the battery is calculated.

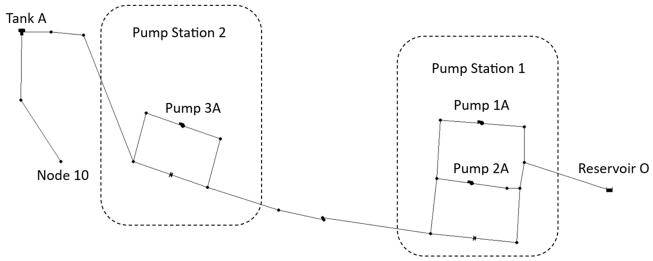

Fig. 2: The topology of Richmond pruned network.

A. Simulation Configuration

The topology of the Richmond pruned network is shown in Figure 2. The network consists of pump station 1 with two identical pumps 1A and 2A, pump station 2 with pump 3A, Reservoir O, Tank A and a demand sector at node 10. [1] provides detailed information about the network including the values of the demand $d_A(k)$, the grid electricity price $p(k)$, the flow into Tank A $q_A(k)$ and the total pumping power $P_p(k)$. $p(k)$ and $d_A(k)$ are both periodic with a period of 24 hours.

$$p(k) = \begin{cases} 0.0679, & 0 \le k \le 16, \\ 0.0241, & 17 \le k \le 23, \end{cases} \tag{17}$$

where the unit is £/kW. The water demands are given by

$$d_A(k) = \alpha(k) d, \tag{18}$$

where d is the constant base demand and $\alpha(k)$ is the demand multiplier shown in Fig. 3. In this case study, the performance of the EMPC is studied for different values of d.

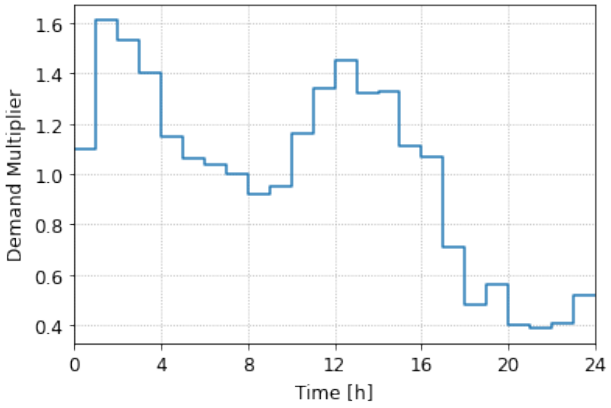

Fig. 3: Demand multipliers for the Richmond pruned network; time 0 represents 7am.

Based on [1], (1), (2), and (5) can be explicitly written as

$$h_A(k+1) = h_A(k) + \frac{T}{S_A}(d_{10}(k) + q_A(k)), \tag{19a}$$

$$q_A(k) = c_1 n_1(k) + c_2 n_2(k) + c_3 n_3(k), \tag{19b}$$

$$P^p(k) = c_4 n_1(k) + c_5 n_2(k) + c_6 n_3(k), \tag{19c}$$

where n_1, n_2, n_3 are the on-off state of fixed speed pumps 1A, 2A, 3A, $S_A = 433.73\,m^2$, $c_1 = 25.21$, $c_2 = 14.65$, $c_3 = 18.02$, $c_4 = 46.32$, $c_5 = 34.61$ and $c_6 = 39.71$. n_1 and n_3 can be used interchangeably because they are identical pumps in the same pump station. $\overline{h}_A = 3.37$ m, $\underline{h}_A = 1.4$ m are the upper and lower bounds of $h_A(k)$. [1] reveals that when $n_1 = 1, n_2 = 1, n_3 = 0$, each unit of power generates significantly lower flow than the other cases. This case is thus not considered when constructing (19b) and (19c). The following constraint is added to the EMPC to ensure $n_1 = 1, n_2 = 1, n_3 = 0$ is not used.

$$n_1(k) \ge n_3(k) \ge n_2(k), \tag{20}$$

A Doyle Fuller Newman (DFN) model of a lithium-ion battery is constructed using PyBaMM to provide realistic battery simulation [13]. The parameters of the simpler battery model in (3) are given as follows: $V^{sb} = 101.2$V, $V^{gb} = 101.5$V, $V^d = 100.9$V, and $C = 7.7$ kAh. The upper limits on the power in (10a) to (10c) are $\overline{P}^{sb} = \overline{P}^{gb} = \overline{P}^d = 120$ kW, and the upper and lower limits on SOC in (8b) are $\overline{\text{SOC}} = 0.85$, $\underline{\text{SOC}} = 0.15$.

A periodic solar power output $P^s(k) = P^s(k+24)$ is artificially generated using (21). The simulation starts at 7 am.

$$P^s(k) = \begin{cases} \left(\cos\left(\frac{\pi k}{6} - \pi\right) + 1\right) P_1, & 0 \le k \le 11, \\ 0, & 12 \le k \le 23. \end{cases} \tag{21}$$

The optimization problem (13)-(15) is implemented in Python with $N = 27$ and $T = 1$ hour - This allows the EMPC to have one-period information of the periodically varying water demand, electricity tariff and solar power. $\gamma_j = 1, j = 1, 2, 3$ is used for the $l_2(k)$ cost. SCIP solver [14] and PySCIPOpt package are used to solve the mixed integer quadratic optimization problem.

B. Results

The simulation results for $d = 30$ L/s and 50 L/s are shown in Fig. 4 and Fig. 5 respectively. As can be seen from Fig. 4(b) and (c), the water level in tank A and the state of charge of the battery go through a cycle where they are filled/charged during the off-peak period and emptied/discharged during the peak period. Fig. 4(d) shows that pump station 1 has one pump running all the time and pump station 2 has one pump running only during the off-peak period. Fig. 4(f) shows that power is only drawn from the grid during the off-peak period after the first peak period. Power is drawn from the grid during the first peak period because the battery is nearly empty at the start of the simulation. Power is only drawn from the gird during the low tariff afterwards because, as illustrated in Fig. 4(e), the battery is charged up during the low tariff and when the solar power is higher than the power required by the pumps. The charged up battery and the solar panel then provide enough power for one pump in pump station 1 to operate during the peak period.

From Fig. 5, Fig. 5(b) and Fig. 5(c) also show that the water level in tank A and the state of charge of the battery

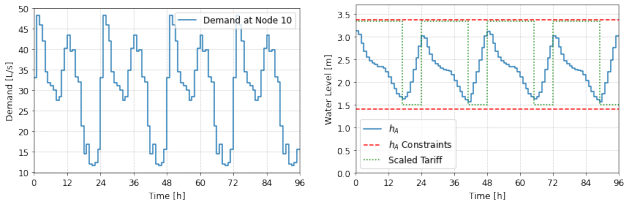

(a) Demand at Node 10

(b) Tank A water level

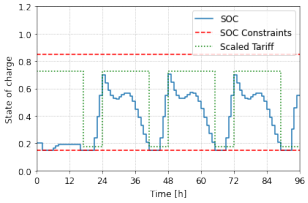

(c) Battery state of charge

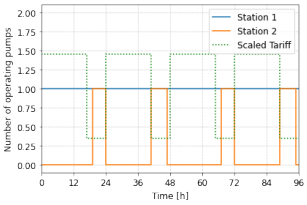

(d) Number of operating pumps

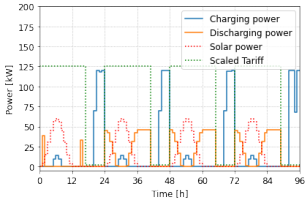

(e) Battery and solar power

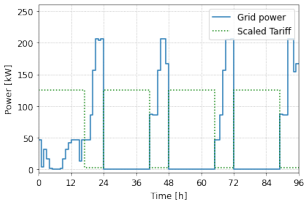

(f) Power drawn from the grid

Fig. 4: Four-day simulation result with $d = 30$ L/s.

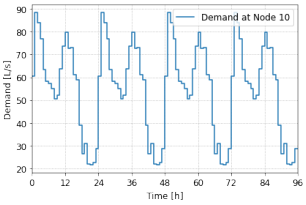

(a) Demand at Node 10

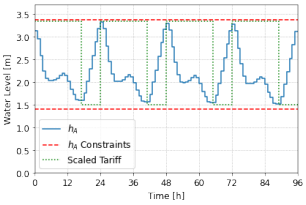

(b) Tank A water level

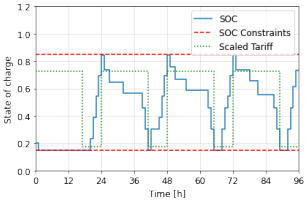

(c) Battery state of charge

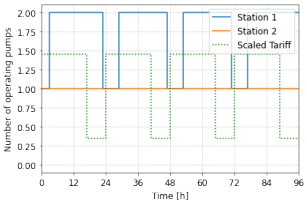

(d) Number of operating pumps

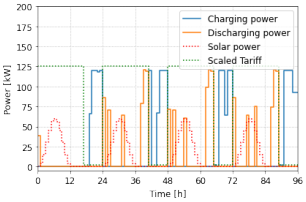

(e) Battery and solar power

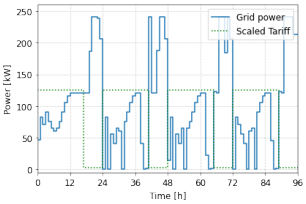

(f) Power drawn from the grid

Fig. 5: Four-day simulation result with $d = 55$ L/s.

also display a cyclic behaviour when the base demand is 55 L/s. Fig. 5(d) shows that the second pump in pump station 1 is turned on early during the peak period to stop the water level in Tank A from dropping below the lower limit at the end of the peak period. One pump in pump station 1 is also powered off before low tariff ends to stop the water level in Tank A from rising above the upper limit. Fig. 5(e) shows that the battery is only charged during the off-peak period and all solar power is transferred directly to the pumps. The amount of power that can be drawn from the grid during off-peak period is limited by the capacity of the battery, the pumps, and Tank A. Increasing the size of the battery and the size of Tank A will allow more electricity to be drawn during the off-peak period instead of the peak period, reducing the cost of electricity but at the expense of an increased infrastructure cost.

When simulating the system with different based demand, one observation is that the difference between the electricity cost when the demand is low, say $d = 10$ L/s and $d = 15$ L/s, is smaller than the difference when the demand is high, say $d = 50$ L/s and $d = 55$ L/s (see right three columns of Table 1). The reason for this is that when the demand is high, the pumps are forced to operate during peak period using expensive electricity; when the demand is low, the pumps can use the low price electricity only and still satisfy the demand. For $d \geq 60$ L/s, the EMPC optimization problem is infeasible because the average demand becomes higher than the flow the pumps can provide, thus d stops at 55 L/s in Table 1.

C. Comparisons

In order to investigate the relative merit of different levels of infrastructure investment when using the proposed controller, we consider the system operating performance under three scenarios: i) a base case without either solar or battery installation; ii) a modified system that only contains solar and iii) further modifications that include both solar and battery storage. The comparison results are shown in Table I. It is observed that a large proportion of electricity cost is saved by the solar panels and the battery when the water demand is low, but drops when the water demand increases because of the limited sizes of the solar panels and the battery. Comparing the result with only the solar panels and the result with both the solar panels and the battery, it is observed that, as expected, the addition of the battery reduces the electricity cost. The reason for this is that the battery can store solar energy and cheap grid electricity to power the pumps during the peak period. Moreover, the battery reduces the number of times pumps are turned ON or OFF during medium and low demands, which translates to prolonged lifetime of the pumps. The reason for this is that, with only the solar panels, the pumps are turned on when the solar is available and when the electricity price is low. However, when the battery is also added, solar energy and cheap electricity from the grid can be stored, allowing the pumps to run longer and turn ON or OFF less often during the peak period. When the demand is high, the number of times the pumps are turned ON or OFF is increased since the pumps need to be turned ON more often to satisfy demand. Moreover, the number of times the pumps are turned ON or OFF is the same for

TABLE I: Simulation result (1) without solar and battery, (2) with only solar, and (3) with both solar and battery

d (L/s)	Without solar and battery		With only solar			With solar and battery		
	Electricity cost (£)	Number of times pumps are turned ON or OFF	Electricity cost (£)	Number of times pumps are turned ON or OFF	Electricity cost saving percentage	Electricity cost (£)	Number of times pumps are turned ON or OFF	Electricity cost saving percentage
5	17.16	8	1.37	6	92%	0	6	100%
10	44.49	15	17.11	12	61%	1.44	8	96%
15	96.69	17	38.60	15	57%	26.53	9	72%
20	152.95	16	70.39	23	54%	52.77	7	65%
25	207.28	15	121.16	20	41%	82.62	3	60%
30	266.17	9	177.36	9	33%	120.42	9	54%
35	319.24	14	224.42	24	30%	167.68	14	47%
40	387.47	15	293.51	15	24%	233.42	15	39%
45	444.01	17	354.46	17	20%	292.32	17	34%
50	522.62	13	421.47	13	19%	365.61	13	30%
55	595.67	9	494.33	9	17%	435.79	9	26%

all three options. The reason is as follows: the first pump runs all the time at high demand, consuming nearly all the solar and battery energy. The schedule of the second and the third pumps, therefore, only depends on the electricity prices and the demands, resulting in approximately the same optimal pumping operation as when no solar or batteries were available.

Although the solar panels and the batteries reduce the electricity cost in WDSs, their infrastructure cost cannot be overlooked. The total reduction in electricity cost over the lifetime of the solar panels and the battery needs to exceed their infrastructure cost to justify including them in the WDSs.

IV. CONCLUSIONS

In this paper, we proposed a novel EMPC framework that minimized the pumping energy cost for a WDS with solar energy and batteries. We formulated the EMPC with a realistic system model, a cost function that closely matches the control objective, and constraints based on limits in operational WDSs. We then applied the proposed EMPC framework in a simulation example. The simulation results showed that the proposed EMPC was able to properly operate the solar panels, the pumps, and the battery to minimize the electricity cost. Moreover, the tank water level and the battery state of charge were kept within their desired operational limits. Therefore, the EMPC design achieves the control objective of minimizing the grid electricity cost while keeping the tank water levels and battery state of charge within the desired ranges. In future work, the stochastic uncertainty in the forecast of water demands, electricity prices, and solar energy output could be considered. Another point worth investigating is formulating the battery state of health into the EMPC to penalize inputs that cause degradation of the battery.

REFERENCES

[1] Y. Wang, K. Too Yok, W. Wu, A. R. Simpson, E. Weyer, and C. Manzie, "Minimizing Pumping Energy Cost in Real-Time Operations of Water Distribution Systems Using Economic Model Predictive Control," *Journal of Water Resources Planning and Management*, vol. 147, no. 7, Apr. 2021.

[2] Y. Wang, J. R. Salvador, D. Muñoz de la Peña, V. Puig, and G. Cembrano, "Economic model predictive control based on a periodicity constraint," *Journal of Process Control*, vol. 68, pp. 226–239, Aug. 2018.

[3] F. K. Pour, V. Puig, and G. Cembrano, "Economic MPC-LPV Control for the Operational Management of Water Distribution Networks," *IFAC-PapersOnLine*, vol. 52, no. 23, pp. 88–93, 2019.

[4] Y. Wang, J. Blesa, and V. Puig, "Robust Periodic Economic Predictive Control based on Interval Arithmetic for Water Distribution Networks," *IFAC-PapersOnLine*, vol. 50, no. 1, pp. 5202–5207, Jul. 2017.

[5] F. Díaz-González, A. Sumper, and O. Gomis-Bellmunt, *Energy Storage in Power Systems*. John Wiley & Sons, 2016.

[6] P. G. V. Sampaio and M. O. A. González, "Photovoltaic solar energy: Conceptual framework," *Renewable and Sustainable Energy Reviews*, vol. 74, pp. 590–601, 2017.

[7] B. Diouf and R. Pode, "Potential of lithium-ion batteries in renewable energy," *Renewable Energy*, vol. 76, pp. 375–380, Apr. 2015.

[8] Aldjia L, Mohamed K, Djalloul A, Chaib A. "Energy management and control of a hybrid water pumping system with storage," *Applied Solar Energy*, vol. 53, pp. 190–198, Sept. 2017.

[9] G. B. Cáceres, A. Ferramosca, P. M. Gata and M. P. Martín, "Model Predictive Control Structures for Periodic ON–OFF Irrigation," *IEEE Access*, vol. 11, pp. 51985-51996, May 2023.

[10] J. B. Rawlings, D. Q. Mayne, and M. Diehl, *Model predictive control: theory, computation, and design*. Santa Barbara, California: Nob Hill Publishing, 2020.

[11] P. K. Ndwali, J. G. Njiri, and E. M. Wanjiru, "Economic Model Predictive Control of Microgrid Connected Photovoltaic-Diesel Generator backup Energy System Considering Demand side Management," *Journal of Electrical Engineering & Technology*, Volume 16, pp. 2297–2312, Jun. 2021.

[12] W. C. Clarke, M. J. Brear, and C. Manzie, "Control of an isolated microgrid using hierarchical economic model predictive control," *Applied Energy*, vol. 280, p. 115960, Dec. 2020.

[13] S. G. Marquis, V. Sulzer, R. Timms, C.P. Please and S.J. Chapman. "An asymptotic derivation of a single particle model with electrolyte". Journal of The Electrochemical Society, 166(15):A3693–A3706, 2019.

[14] K. Bestuzheva, et al., *SCIP Optimization Suite 8.0*. Available at Optimization Online and as ZIB-Report 21-41, Dec. 2021.

[15] Y. Wang, "Water System Management," GitHub, Sep. 01, 2020. https://github.com/dryewang/watersystem.